Article ID: 1000-7032(2025)07-1232-09

Surface Chemistry Engineering of Gold Nanoclusters Toward High-efficiency White Light Emission

WANG Kunyu, WANG Xue, YANG Yi, ZHONG Yuan, DONG Weinan, LU Min, WU Zhennan*, ZHANG Yu*, BAI Xue*

(*State Key Laboratory of Integrated Optoelectronics, JLU Region and College of Electronic Science and Engineering, Jilin University, Changchun* 130012, *China*)

* *Corresponding Authors, E-mail: wuzn@jlu. edu. cn; yuzhang@jlu. edu. cn; baix@jlu. edu. cn*

Abstract: Photoluminescence (PL) is one of the most important properties of metal nanoclusters (NCs). Achieving efficient white light emission in metal NCs with a precise structures is important for practical applications but remains a great challenge. Here, we report the efficient white emission from Au_{10} NCs by elaborately deploying the surface chemistry engineering strategy. Specifically, the bis-aldehyde ligands of 4-hydroxyisophthalaldehyde (HOA) are decorated on the surface of $Au_{10}(SG)_{10}$ NCs (glutathione denoted as SG) through the cross-linking reaction of imine bonds (—CH═N—). The combination of 477 nm blue emission from HOA ligands and 620 nm orange-yellow emission from $Au_{10}(SG)_{10}$ NCs generates white-light emission in HOA-$Au_{10}(SG)_{10}$ NCs in the solvent mixture of ethanol and water. More importantly, dynamic color tuning from blue light to yellow light is achieved by controlling the volume fraction of ethanol in the solvent mixture. In addition, the as-formed imine bonds significantly improve the structural rigidity of HOA-$Au_{10}(SG)_{10}$ NCs, resulting in the 51. 2% absolute photoluminescence quantum yield (PLQY) of white emission. The present study exemplifies the paradigm to control the emission color and improve the PLQY of metal NCs through rational surface chemistry engineering.

Key words: metal nanoclusters; white-light emission; electron transfer

CLC number: O482. 31 **Document code**: A

DOI: 10. 37188/CJL. 20250073 **CSTR**: 32170. 14. CJL. 20250073

通过表面化学工程实现高效白光发射的金纳米团簇

汪琨钰, 王 雪, 杨 毅, 钟 圆, 董伟男, 陆 敏, 武振楠*, 张 宇*, 白 雪*

(吉林大学 电子科学与工程学院, 集成光电子全国重点实验室吉林大学实验区, 吉林 长春 130012)

摘要: 光致发光(PL)是金属纳米团簇(NCs)最重要的性质之一。在结构精确的金属纳米团簇中实现高效的白光发射对实际应用具有重要意义,但仍然是一个巨大的挑战。本文通过精心部署表面化学工程策略,报道了Au_{10}纳米团簇的高效白色发射。具体来说,4-羟基间苯二醛(HOA)的双醛配体通过亚胺键(—CH═N—)的交联反应修饰在$Au_{10}(SG)_{10}$ NCs(SG为谷胱甘肽)表面。在乙醇和水的混合溶剂中,HOA配体的477 nm蓝光和$Au_{10}(SG)_{10}$ NCs的620 nm橙黄光组合产生了HOA-$Au_{10}(SG)_{10}$NCs的白光发光。更重要的是,通过控制溶剂混合物中乙醇的体积分数,实现了从蓝光到黄光的动态颜色调节。此外,形成的亚胺键显著提高了HOA-$Au_{10}(SG)_{10}$ NCs的结构刚性,使其白色发光的绝对光致发光量子产率(PLQY)达到51.2%。本研究为通过表面化学工程合理地控制金属NCs的发射颜色和提高PLQY提供了研究方向。

关 键 词: 金属纳米团簇; 白光发光; 电子转移

收稿日期: 2025-03-12; **修订日期**: 2025-03-30

基金项目: 国家自然科学基金(T2325015,U21A2068,61935009,12174151)

Supported by National Natural Science Foundation of China(T2325015,U21A2068,61935009,12174151)

1 Introduction

In the current information age, the development of white-light-emitting materials is becoming increasingly important because of their potential applications in lighting and displays[1-3]. The ideal white-light-emitting materials require an emission band that covers the entire visible spectral region to achieve a high color rendering index (R_a). This requires multiple emitting centers within the luminescent materials and a corresponding dynamically adjustable emission intensity based on the tunable energy/electron transfer channels. So far, various luminescent materials, including semiconductor quantum dots, lanthanides co-doped solid phosphors, and single-molecule organic emitters, have been investigated and demonstrated to be potential white-light-emitting materials[4-6]. However, the inherent shortcomings of these luminescent materials make the white emission from them suffer from the low photoluminescence quantum yield (PLQY) and poor color tunability[7-8]. It, therefore, remains challenging to prepare highly efficient and dynamically color-tunable white-light-emitting materials.

Metal nanoclusters (NCs) are typically composed of few-to hundred-metal-atom aggregates protected by an organic ligand monolayer, which have been modeled by a "divide-and-protect" concept[9-11]. PL is one of the most important properties of metal NCs[12]. The hierarchical structure of metal NCs (including metal core, staple motifs, and surface ligands) contributes to the diverse PL types (including singlet-state fluorescence, triplet-state phosphorescence, thermally activated delayed fluorescence, defect-state emission, *etc.*)[13-15]. The PL of metal NCs exhibits a strong quantum confinement effect, leading to a tunable emission band covering the visible and near-infrared region. Therefore, luminescent metal NCs are promising candidates to exhibit white-light emission with high efficiency and color tunability. Nevertheless, very limited success has been achieved due to the remaining challenges[16-18]. First, the enormous difficulty lies in realizing multi-peak emission in metal NCs[19-21]. Second, unclear energy/electron transfer laws between multiple luminescent centers in metal NCs hampered the customization of single-component white light. Third, the non-radiative relaxation of metallic NCs makes efficient white light emission difficult[22-24]. Therefore, tremendous challenges remain in preparing atomically structurally precise white-light-emitting metal NCs with high PLQY to fully understand the structural origin of white emission and the accurate structure-property relationship in the process of luminescence color regulation.

Herein, we report the efficient white emission with customized emission color from atomically precise metal NCs, by deploying the surface chemistry engineering strategy[25-26]. Especially, atomically precise $Au_{10}(SG)_{10}$ NCs are employed as model NCs to afford 620 nm orange-yellow emission in ethanol solution. In addition, the surface ligand was chosen to be bis-aldehydes molecule of 4-hydroxyisophthalaldehyde (HOA) containing two aldehyde groups (—CHO) that can react with the amino group ($—NH_2$) in the terminal of the glutathione ligands to form imine bonding (—CH═N—). The resultant HOA-$Au_{10}(SG)_{10}$ NCs synthesized by surface cross-linking reaction show efficient white emission (51.2% PLQY) in 94% ethanol with two emission centers located at 477 nm and 620 nm contributed from surface HOA ligands and $Au_{10}(SG)_{10}$ NCs, respectively. Femtosecond-transient absorption (TA) measurements indicate that the electron transfer from surface HOA ligands to inner $Au_{10}(SG)_{10}$ NCs is formed after anchoring the HOA ligands. Finally, dynamic color tuning from blue to yellow light is achieved by controlling the volume fraction of ethanol in the solvent mixture.

2 Experiment

2.1 Materials

Hydrogen tetrachloroaurate (Ⅲ) trihydrate ($HAuCl_4 \cdot 3H_2O$, ≥49.0%) was purchased from Sigma Aldrich. 4-Hydroxyisophthalaldehyde (HOA, 98%), and sodium hydroxide (NaOH, 96%) were purchased from Energy Chemical (Shanghai, China). Carbon monoxide (CO, 99.99%) was provided by Changchun Juyang Gas Co. Ethanol (99.7%) was obtained from Fuyu Fine Chemical Co. All chemicals were used as received without additional purification. Dialysis Bags

(MD55-3500) were obtained from Hunan Yibo Biotechnology Co. Ultrapure Millipore water (18.2 MΩ) was used throughout the experiments to dissolve regents and as reaction media.

2.2 Synthesis of $Au_{10}(SG)_{10}$ NCs

In a typical synthesis of white-emitting Au NCs, 5 mL aqueous solutions of $HAuCl_4$ (50 mmol/L) and 10 mL GSH (50 mmol/L) were added to 235 mL of ultrapure water under 600 r/min stirring at room temperature. The greenish-yellow solution (the original color of the $HAuCl_4$ solution) quickly turned white with the appearance of precipitation, implying the formation of Au(Ⅰ)-thiolate complexes. After 2 min, the pH of the aqueous solution was carefully tuned to 7.0 by dropping in NaOH solution (1 mol/L), and the solution transformed from white to colorless. One bar of CO gas was bubbled through the reaction solution for 2 min, after which the solution was sealed airtight and stirred at 600 r/min at room temperature. After 24 h, the crude products were collected and lyophilized into powder.

2.3 Synthesis of HOA-$Au_{10}(SG)_{10}$ NCs

Typically, 40 μL aqueous solution of $Au_{10}(SG)_{10}$ NCs (5 mmol/L) and 80 μL aqueous solution of HOA (1 mmol/L) were added to 1.88 mL phosphate buffer (20 mmol/L, pH=7.0). The mixture was allowed to react for 0.5 h at room temperature and 1 h dialysis experiment. Then stored in a 4 ℃ refrigerator for further use.

2.4 Characterizations

^{1}H-nuclear magnetic resonance (^{1}H-NMR) were performed with an AS 400 MHz (Q. One Instruments Ltd.) system. $CDCl_3$ was used as a solvent for all ^{1}H-NMR measurements. UV-Vis absorption spectra were recorded on the Shimadzu UV-1900i spectrometer. PL and PL excitation (PLE) spectra were measured on a Hitachi F-4700 spectrometer with excitation. FT-IR spectra were collected on a Nicolet Is50 spectrometer (Thermo Fisher) using a single attenuated total reflectance accessory at 400–4 000 cm^{-1} scanning range. The PLQY of $Au_{10}(SG)_{10}$ and HOA-$Au_{10}(SG)_{10}$ NCs samples in water-ethanol mixed solution were measured and calculated on an FLS1000 spectrofluorometer (Edinburgh Instruments Ltd.) attached with an integrating sphere coating with a reflective $BaSO_4$ layer. Femtosecond-transient absorption (fs-TA) measurement was performed on a commercial Ti: Sapphire laser system (Spitfire Spectra-Physics). The system is equipped with femtosecond pulsed lasers in the ultraviolet to near-infrared wavelength bands, regenerative amplifier system (Spitfire, Spectra-Physics), electronically delayed supercontinuum light source with a sub-nanosecond pulse duration (EOS, Ultrafast Systems), and dual spectrometers with array detectors.

3 Results and Discussion

The $Au_{10}(SG)_{10}$ NCs are attractive in the lighting and biological fields due to their unique PL properties, excellent photostability, and biocompatibility[27-30]. Based on the reported carbon monoxide (CO) reduction method, molecularly pure $Au_{10}(SG)_{10}$ NCs can be easily synthesized[27]. Its precise atomic structure of $Au_{10}(SG)_{10}$ NCs has been reported[28], consisting of two interspersed cyclic $Au_5(SG)_5$ pentamers (Fig. 1(a)). The as-synthesized $Au_{10}(SG)_{10}$ NCs show two characteristic absorption features in an aqueous solution peaking at 330 nm and 370 nm, respectively (Fig. S1). We found that poor solvents, such as ethanol, can lead to aggregation-induced emission (AIE) of $Au_{10}(SG)_{10}$ NCs because the polarity of ethanol (dielectric constant ~25.3) is weaker than that of water (dielectric constant~80.1), and the degree of cluster aggregation is related to the volume fraction of ethanol (*i. e.*, f_e, $f_e=v_{ethanol}/v_{ethanol+water}$) in the ethanol-water mixture[13, 21, 31-32]. In the mixed water-ethanol solution, the absorption features of $Au_{10}(SG)_{10}$ NCs remained unchanged, which indicates that the structure of $Au_{10}(SG)_{10}$ NCs maintained. However, a distinct emission peak at 620 nm is observed (Fig. 1(b)), which is the typical AIE property of $Au_{10}(SG)_{10}$ NCs[33].

To construct white light emission and increase PLQY of $Au_{10}(SG)_{10}$ NCs, HOA ligands with a double aldehyde group (—CHO) were anchored on the surface of $Au_{10}(SG)_{10}$ NCs in leveraging of the imine bonds (—CH═N—) through bis-Schiff base linkage reacted between aldehyde group in HOA ligands and amino group in $Au_{10}(SG)_{10}$ NCs (Fig. 2)[34]. The obtained HOA-$Au_{10}(SG)_{10}$ NCs show bright

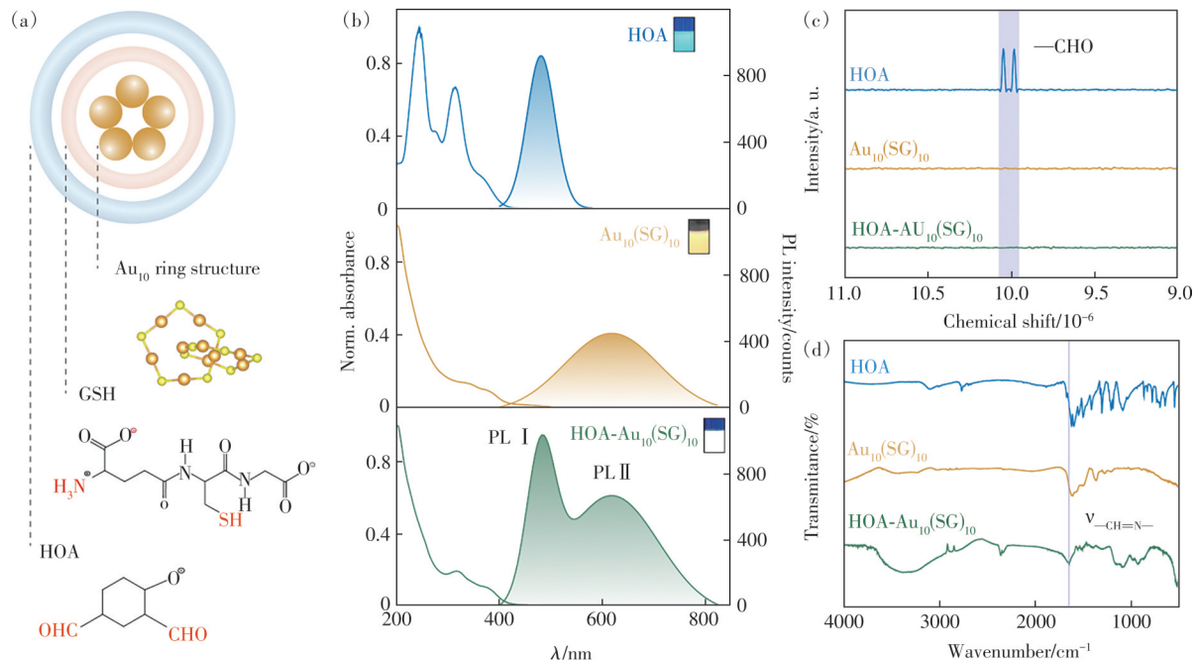

Fig. 1　(a) Schematic structure of HOA-$Au_{10}(SG)_{10}$ NCs. (b) UV-Vis absorption spectra, PL spectra, and a digital photograph of solutions excited at 375 nm. ^{1}H-NMR (c) and FT-IR spectra (d) of pure HOA ligands (top), $Au_{10}(SG)_{10}$ NCs (middle), and HOA-$Au_{10}(SG)_{10}$ NCs (bottom)

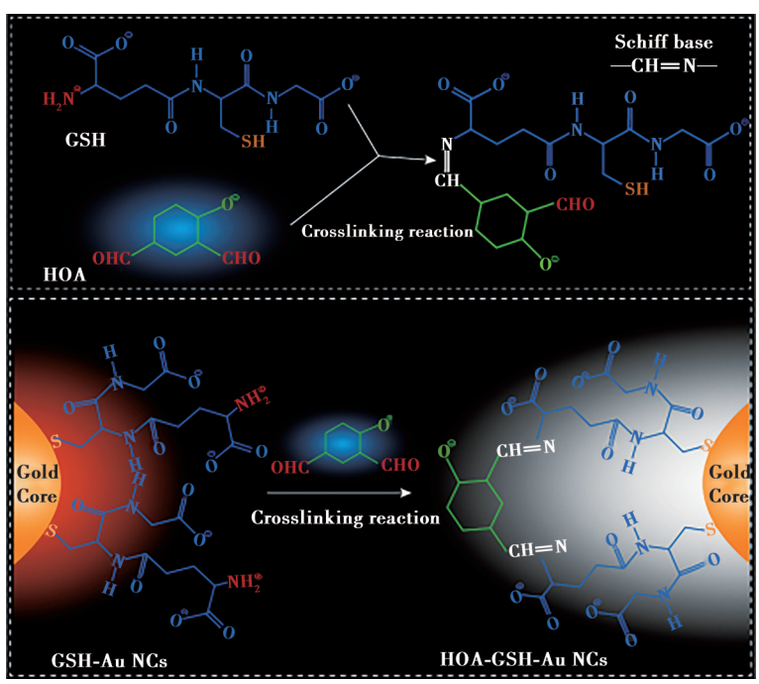

Fig. 2　Schematic illustration of the construction of white-light-emitting HOA-$Au_{10}(SG)_{10}$ NCs through a surface chemistry engineering strategy

white-light emission with a Commission Internationale de L'Éclairage (CIE) chromaticity coordinates of (0.29, 0.3) under 375 nm excitation in 94% ethanol solution (Fig. S2). Two distinct emission peaks at 477 nm and 620 nm derive from the characteristic emission of HOA ligands and $Au_{10}(SG)_{10}$ NCs, respectively (Fig. 1(b)). The absolute PLQY of HOA-$Au_{10}(SG)_{10}$ NCs was recorded to reach 51.2% at room temperature with uniform photoluminescent distribution and high stability at 4 ℃ (Fig. S3-4). In addition, we found that the emission color of HOA-$Au_{10}(SG)_{10}$ NCs can be dynamically adjusted from blue to white and finally to yellow by adjusting the ratio of ethanol to water (Fig. 3(a))[33].

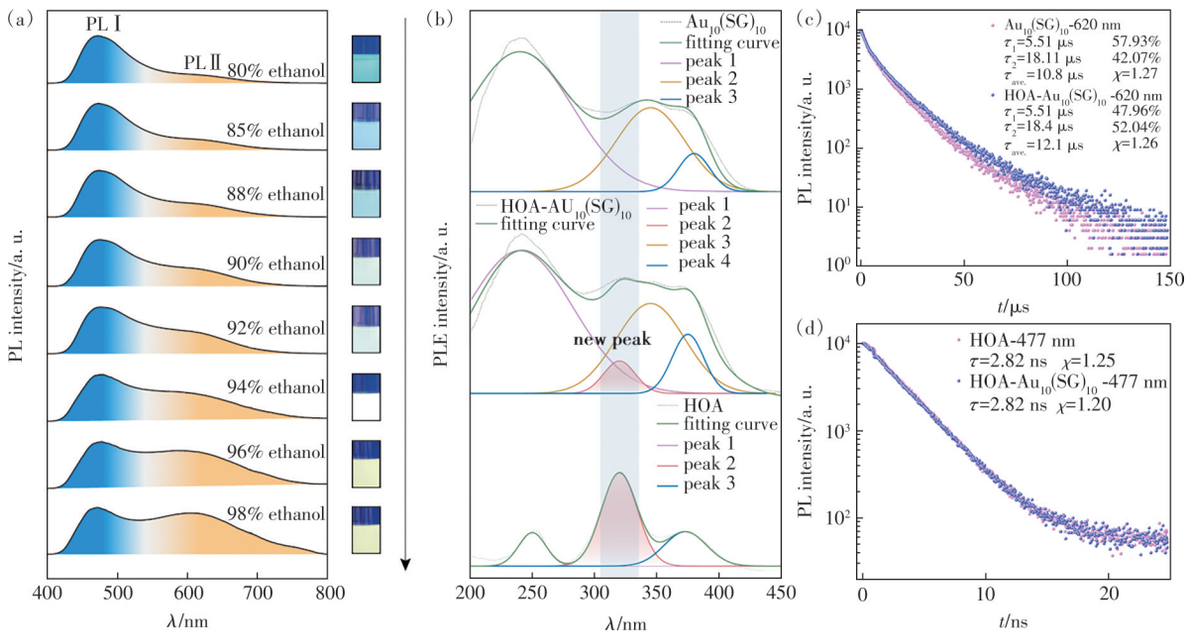

Fig. 3 (a)The emission intensity variation curves and a digital photograph for solutions excited at 375 nm with ethanol concentrations ranging from 80% to 98% are presented. (b)The PLE deconvolution spectra of $Au_{10}(SG)_{10}$(top) and HOA-$Au_{10}(SG)_{10}$ NCs (middle) tested at 620 nm. The PLE deconvolution spectra of HOA ligands(bottom) tested at 477 nm. (c)Comparison of the PL decay of $Au_{10}(SG)_{10}$ and HOA-$Au_{10}(SG)_{10}$ NCs upon 375 nm excitation and 620 nm monitoring. (d)Comparison of the PL decay of HOA ligands and HOA-$Au_{10}(SG)_{10}$ NCs upon 375 nm excitation and 477 nm monitoring

^{1}H-NMR and FT-IR measurements were carried out to prove the successful chelation of HOA ligands on the surface of $Au_{10}(SG)_{10}$ NCs. As shown in Fig. 1(c), the ^{1}H-NMR of pure HOA ligands has two sharp peaks at about 10.0×10^{-6}, corresponding to two —CHO groups with different chemical environments (Fig. S5). However, the two peaks of —CHO groups disappeared in the ^{1}H-NMR of HOA-$Au_{10}(SG)_{10}$ NCs, indicating that the accomplished dehydration and condensation reactions of the —CHO groups in HOA ligands with the —NH_2 groups in the $Au_{10}(SG)_{10}$ NCs to form imine bonds. The presence of imine bonds was further demonstrated by the FT-IR spectra of HOA-$Au_{10}(SG)_{10}$ NCs where the appearance of stretching vibration at 1 652 cm^{-1} can be rationally assigned to the imine bonds (Fig. 1(d))[34]. Consequently, the HOA ligands were successfully anchored to the surface of $Au_{10}(SG)_{10}$ NCs through the formation of imine bonds, rather than through simple physical mixing.

To investigate the electronic interactions between HOA and $Au_{10}(SG)_{10}$ NCs, the PLE spectra of PL Ⅰ and PL Ⅱ of HOA ligands, $Au_{10}(SG)_{10}$, and HOA-$Au_{10}(SG)_{10}$ NCs were recorded (Fig. 3(b)). Surprisingly, a new excitation peak at 320 nm was observed in the PLE spectrum of PL Ⅱ of HOA-$Au_{10}(SG)_{10}$ NCs compared to that of $Au_{10}(SG)_{10}$ NCs. This additional PLE peak is consistent with the PLE peak of the HOA ligands, which suggests a possible transfer channel of excited state electrons from HOA ligands to $Au_{10}(SG)_{10}$ NCs. This phenomenon coincides with the electron transfer previously observed in Au NCs with dual emission[21]. In addition, the emission peak position of HOA ligands overlaps very little with the absorption peak position of $Au_{10}(SG)_{10}$ NCs, and the lifetime of the HOA remains unchanged. Therefore, it can be reasonably concluded that the energy transfer between PL Ⅰ and PL Ⅱ does not occur, but rather an electron transfer from PL Ⅰ to PL Ⅱ.

Next, the electron transfer process between HOA and $Au_{10}(SG)_{10}$ NCs was monitored dynamically by varying the molar ratio of $Au_{10}(SG)_{10}$ NCs and HOA during the synthesis process. With the increase of the proportion of $Au_{10}(SG)_{10}$ NCs, the emission intensity of PL Ⅱ increases significantly (Fig. S6). To exclude the effect of PL Ⅱ on PL Ⅰ, a series of HOA-$Au_{10}(SG)_{10}$ NCs excitations were subjected to deconvolution. It was found that the emission intensity of PL Ⅰ gradually decreases and eventually

remains constant, with the increase of the proportion of $Au_{10}(SG)_{10}$ NCs. This result can be attributed to the saturation of the reaction between HOA and $Au_{10}(SG)_{10}$ NCs, which ultimately leads to the maximization of electron transfer from HOA to $Au_{10}(SG)_{10}$ NCs. Similarly, the characteristic PLE peaks derived from HOA were observed in the PLE spectra of PL Ⅱ of a series of HOA-$Au_{10}(SG)_{10}$ NCs (Fig. S7). To gain insight into the changes in the PL decay pathway, the PL lifetimes of HOA ligands, $Au_{10}(SG)_{10}$ and HOA-$Au_{10}(SG)_{10}$ NCs were obtained by time-resolved PL spectroscopy (Fig. 3(c)-(d) and Fig. S8). The PL lifetime of PL Ⅰ in HOA-$Au_{10}(SG)_{10}$NCs (τ =2.82 ns) is consistent with that of HOA (τ =2.82 ns). However, the photoluminescence lifetime of PL Ⅱ in HOA-$Au_{10}(SG)_{10}$ NCs ($\tau_{ave.}$ =12.1 μs) was increased compared to that of $Au_{10}(SG)_{10}$ NCs ($\tau_{ave.}$ =10.8 μs). By performing a biexponential fit to the photoluminescence lifetime of PL Ⅱ of Au NCs, it was found that the effective suppression of non-radiation relaxation and enhancement of luminescence. These results demonstrate that emission bands of PL Ⅰ and PL Ⅱ in white-light-emitting HOA-$Au_{10}(SG)_{10}$ NCs originate from the singlet-state fluorescent in HOA ligands and triplet-state phosphorescence in $Au_{10}(SG)_{10}$ NCs, respectively.

In addition to the PLE spectra, fs-TA was employed to investigate the potential electron transfer processes in white-emitting HOA-$Au_{10}(SG)_{10}$ NCs. The fs-TA maps of $Au_{10}(SG)_{10}$ NCs, HOA, and HOA-$Au_{10}(SG)_{10}$ NCs revealed varying degrees of excited state absorption (ESA) upon 340 nm laser pulses pumping (Fig. S9). The fs-TA profile map of $Au_{10}(SG)_{10}$ NCs exhibits two ESA bands at 420 nm and 540 nm, while the HOA displays three ESA bands at 460 nm, 480 nm, and 520 nm (Fig. 4(a)-(b)). The fs-TA map of HOA-$Au_{10}(SG)_{10}$ NCs has a new ESA band at 580 nm compared to that of $Au_{10}(SG)_{10}$ NCs (Fig. 4(c))[35]. This new ESA band is attributed to the transfer of excited state electrons from HOA to $Au_{10}(SG)_{10}$ NCs. Subsequently, we conducted lifetime fits to the decay kinetics at 420 nm of $Au_{10}(SG)_{10}$ NCs and HOA-$Au_{10}(SG)_{10}$ NCs. It is found that three decay components can be fitted out in the ESA kinetics of $Au_{10}(SG)_{10}$ NCs (Fig. 4(d)). Firstly, the excited state electron undergoes an ultrafast internal transition (IC) from S_n

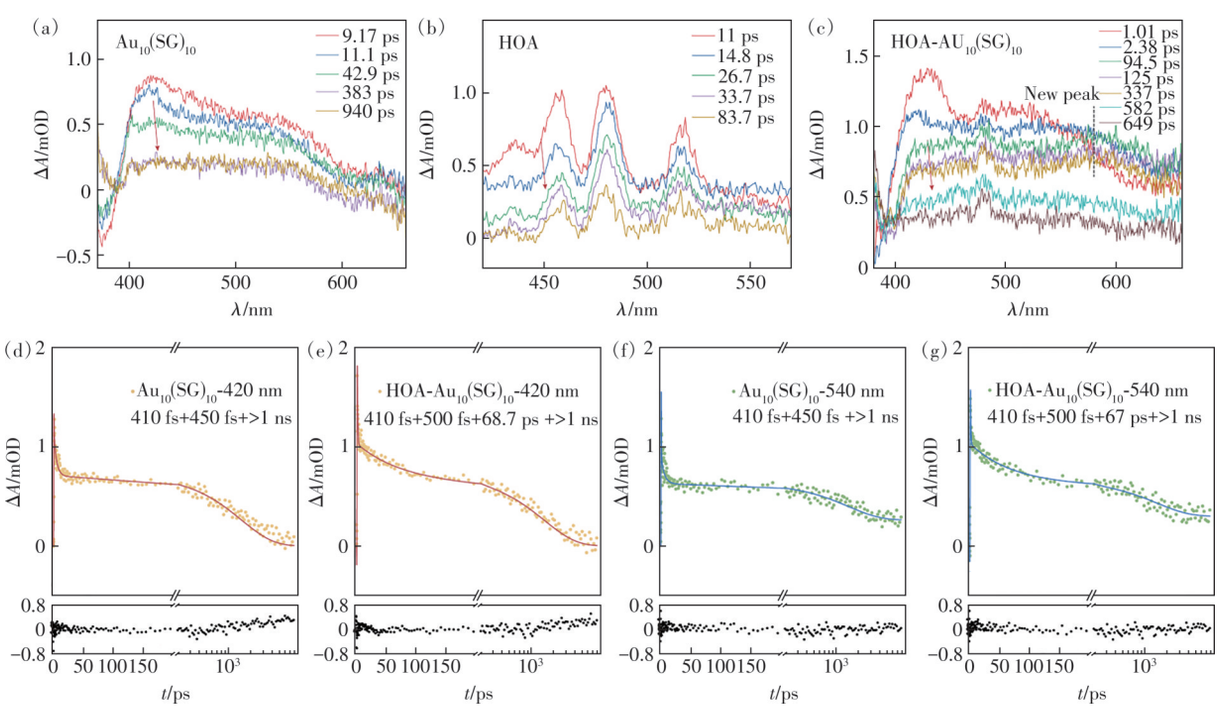

Fig. 4　(a)-(c) The fs-TA profile of $Au_{10}(SG)_{10}$ NCs, HOA, and HOA-$Au_{10}(SG)_{10}$ NCs at different time delays. ESA kinetic decay and fitting residuals at 420 nm ((d)-(e)) and 540 nm ((f)-(g)) within 8 ns (from left to right: $Au_{10}(SG)_{10}$ and HOA-$Au_{10}(SG)_{10}$)

to the S_1 state ($S_n \rightarrow S_1$, 410 fs). It then followed the structural relaxation (VR) process in S_1 (450 fs). Finally, a radiative relaxation occurs from the low excited state of S_1 to the ground state ($T_1 \rightarrow S_0$, >1 ns). In contrast, four decay components were fitted out in the ESA kinetics of HOA-$Au_{10}(SG)_{10}$ NCs (Fig. 4(e)). In addition to ultrafast IC relaxation (410 fs), VR in S_1 (500 fs), and radiative relaxation (>1 ns), an additional decay process (~tens of ps) appears which can be rationally assigned to the electron transfer process from HOA ligands to $Au_{10}(SG)_{10}$ NCs[36]. In a series of HOA-$Au_{10}(SG)_{10}$ NCs with different concentrations of HOA, the time constant of electron transfer less gradually with increasing concentration of HOA (from 68.7 ps to 34.6 ps and 9.6 ps), indicating that electron transfer undergoes more quickly (Fig. 4(e) and Fig. S10)[21]. In addition, the ESA band at 540 nm was also subjected to fit. The decay components are nearly identical to those observed at 420 nm (Fig. 4(f)-(g) and Fig. S11). Furthermore, it is noteworthy that the time constant of the VR process increases from 450 fs to 500 fs with the increase in the concentration of HOA. This result can be attributed to the reduced distance between the core and shell caused by the formation of the Schiff base linkage which can significantly suppress the vibrations of cyclic $Au_5(SG)_5$ pentamers and therefore decrease the non-radiative relaxation in HOA-$Au_{10}(SG)_{10}$ NCs[34].

Combining the results of steady-state PLE, PL spectroscopy, and fs-TA measurements, we provide a plausible explanation for the efficient white light emission Au NCs achieved by surface chemical modification. Fig. 5 illustrates the corresponding excited-state electron dynamics. The ground state electrons can be excited to the excited state (S_n) by the high-energy (340 nm) pump. The excited electrons first undergo ultrafast IC relaxation in hundreds of femtoseconds, resulting in the cooling of hot electrons to the S_1 state. In $Au_{10}(SG)_{10}$ NCs, excited-state electrons in the lowest energy of the S_1 state first relax to the lowest T_1 state *via* a non-radiative intersystem crossing (ISC) process and then undergo a $T_1 \rightarrow S_0$ relaxation to emit 620 nm phosphorescence. The excited electrons in HOA-$Au_{10}(SG)_{10}$ NCs experience the same relaxations to reach the lowest energy S_1 state. The difference is that the T_1 state also receives excited-state electrons from the S_1 state of the HOA ligands. In addition to this transition, the excited-state electrons in the S_1 state of the HOA ligands can directly relax to the ground state of S_0 ($S_1 \rightarrow S_0$), accompanied by 477 nm blue fluorescence from HOA ligands. Finally, the combination of 477 nm blue fluorescence from HOA ligands and 620 nm orange-yellow phosphorescence from $Au_{10}(SG)_{10}$ NCs achieves white-light emission in HOA-$Au_{10}(SG)_{10}$ NCs.

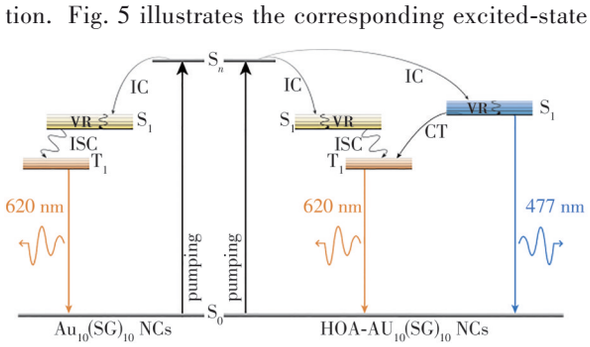

Fig. 5 Schematic illustration of the excited-state electron dynamics in $Au_{10}(SG)_{10}$ and HOA-$Au_{10}(SG)_{10}$ NCs

4 Conclusion

In summary, we successfully synthesized single-component white-light-emitting HOA-$Au_{10}(SG)_{10}$ NCs with a high absolute PLQY of 51.2% through a surface ligand engineering strategy. HOA-$Au_{10}(SG)_{10}$ NCs exhibit two emission peaks located at 477 nm and 620 nm, respectively. The emission color of HOA-$Au_{10}(SG)_{10}$ NCs can be dynamically tuned from blue to yellow. It was demonstrated that the imine bonds formed between HOA ligands and $Au_{10}(SG)_{10}$ NCs significantly increase the structural rigidity of $Au_{10}(SG)_{10}$ NCs, which contributes to the significant PLQY enhancement. In addition, there is a unique excited state electron transfer behaviour from HOA ligands to $Au_{10}(SG)_{10}$ NCs. This study gives deep insights into the relationship between the structural characteristics of metal NCs and their white emission properties. The proposed surface ligand engineering strategy can be extended to other photoluminescent metal nanoclusters with

core-shell structures, providing synthetic routes to fields such as optical sensing and light-emitting displays.

Supplementary Information and Response Letter are available for this paper at: http://cjl.lightpublishing.cn/thesisDetails#10.37188/CJL.20250073

References:

[1] SETLUR A A, LYONS R J, MURPHY J E, *et al*. Blue light-emitting diode phosphors based upon oxide, oxyhalide, and halide hosts [J]. *ECS J. Solid State Sci. Technol.*, 2013, 2(2): R3059-R3070.

[2] SMET P F, PARMENTIER A B, POELMAN D. Selecting conversion phosphors for white light-emitting diodes [J]. *J. Electrochem. Soc.*, 2011, 158(6): R37-R54.

[3] YIN M J, PAN T, YU Z W, *et al*. Color-stable WRGB emission from blue OLEDs with quantum dots-based patterned down-conversion layer [J]. *Org. Electron.*, 2018, 62: 407-411.

[4] GATHER M C, KÖHNEN A, MEERHOLZ K, *et al*. White organic light-emitting diodes [J]. *Adv. Mater.*, 2010, 23(2): 233-248.

[5] HASSAN Z, ABD H R, ALSULTANY F H, *et al*. Investigation of sintering temperature and Ce^{3+} concentration in YAG: Ce phosphor powder prepared by microwave combustion for white-light-emitting diode luminance applications [J]. *Mater. Chem. Phys.*, 2019, 229: 22-31.

[6] KAMTEKAR K T, MONKMAN A P, BRYCE M R. Recent advances in white organic light-emitting materials and devices (WOLEDs) [J]. *Adv. Mater.*, 2010, 22(5): 572-582.

[7] XU B J, WU H Z, CHEN J R, *et al*. White-light emission from a single heavy atom-free molecule with room temperature phosphorescence, mechanochromism and thermochromism [J]. *Chem. Sci.*, 2017, 8(3): 1909-1914.

[8] MALAKAR P, MODAK D, PRASAD E. Pure white light emission from organic molecules using solvent induced selective self-assembly [J]. *Chem. Commun.*, 2016, 52(23): 4309-4312.

[9] YAO Q F, LIU L M, MALOLA S, *et al*. Supercrystal engineering of atomically precise gold nanoparticles promoted by surface dynamics [J]. *Nat. Chem.*, 2023, 15(2): 230-239.

[10] MATUS M F, HÄKKINEN H. Understanding ligand-protected noble metal nanoclusters at work [J]. *Nat. Rev. Mater.*, 2023, 8(6): 372-389.

[11] JIN R C, ZENG C J, ZHOU M, *et al*. Atomically precise colloidal metal nanoclusters and nanoparticles: fundamentals and opportunities [J]. *Chem. Rev.*, 2016, 116(18): 10346-10413.

[12] KANG X, ZHU M Z. Tailoring the photoluminescence of atomically precise nanoclusters [J]. *Chem. Soc. Rev.*, 2019, 48(8): 2422-2457.

[13] LUO Z T, YUAN X, YU Y, *et al*. From aggregation-induced emission of Au(I)-thiolate complexes to ultrabright Au(0)@Au(I)-thiolate core-shell nanoclusters [J]. *J. Am. Chem. Soc.*, 2012, 134(40): 16662-16670.

[14] ZHOU M, SONG Y B. Origins of visible and near-infrared emissions in $[Au_{25}(SR)_{18}]^-$ nanoclusters [J]. *J. Phys. Chem. Lett.*, 2021, 12(5): 1514-1519.

[15] SI W D, ZHANG C K, ZHOU M, *et al*. Two triplet emitting states in one emitter: near-infrared dual-phosphorescent Au_{20} nanocluster [J]. *Sci. Adv*, 2023, 9(13): eadg3587.

[16] ZHANG Y J, FENG N, ZHOU S J, *et al*. Fluorescent nanocomposites based on gold nanoclusters for metal ion detection and white light emitting diodes [J]. *Nanoscale*, 2021, 13(7): 4140-4150.

[17] SUN P P, WANG Z, SUN D, *et al*. pH-Guided self-assembly of silver nanoclusters with aggregation-induced emission for rewritable fluorescent platform and white light emitting diode application [J]. *J. Colloid Interface Sci.*, 2020, 567: 235-242.

[18] XIE H Y, WANG Y Q, ZHANG N, *et al*. Solvent-induced self-assembly of silver nanoclusters for white-light-emitting diodes and temperature sensing [J]. *ACS Appl. Nano Mater.*, 2024, 7(1): 1009-1018.

[19] ZHONG Y, ZHANG J W, LI T T, *et al*. Suppression of kernel vibrations by layer-by-layer ligand engineering boosts photoluminescence efficiency of gold nanoclusters [J]. *Nat. Commun.*, 2023, 14(1): 658.

[20] ZHANG S S, HAVENRIDGE S, ZHANG C K, *et al*. Sulfide boosting near-unity photoluminescence quantum yield of silver nanocluster [J]. *J. Am. Chem. Soc.*, 2022, 144(40): 18305-18314.

[21] CHANG H, KARAN N S, SHIN K, *et al*. Highly fluorescent gold cluster assembly [J]. *J. Am. Chem. Soc.*, 2021, 143(1): 326-334.

[22] WANG Z X, GAO H, LI X Q, *et al*. Interface engineering of copper nanocluster assemblies with white-light emission [J]. *Adv. Funct. Mater.*, 2023, 33(42): 2305209.

[23] PYO K, XU H M, HAN S M, *et al*. Synthesis and photophysical properties of light-harvesting gold nanoclusters fully functionalized with antenna chromophores [J]. *Small*, 2021, 17(27): 2004836.

[24] ZHONG Y, WANG X, LI T T, *et al*. White-emitting gold nanocluster assembly with dynamic color tuning [J]. *Nano Lett.*, 2024, 24(23): 6997-7003.

[25] TIAN W D, SI W D, HAVENRIDGE S, *et al*. Biomimetic crystallization for long-pursued-COOH-functionalized gold nanocluster with near-infrared phosphorescence [J]. *Sci. Bull.*, 2024, 69(1): 40-48.

[26] SI W D, ZHANG C K, ZHOU M, *et al*. Arylgold nanoclusters: phenyl-stabilized Au_{44} with thermal-controlled NIR single/dual-channel phosphorescence [J]. *Sci. Adv.*, 2024, 10(6928): eadm6928.

[27] YU Y, CHEN X, YAO Q F, *et al*. Scalable and precise synthesis of thiolated $Au_{10\text{-}12}$, Au_{15}, Au_{18}, and Au_{25} nanoclusters *via* pH controlled CO reduction [J]. *Chem. Mater.*, 2013, 25(6): 946-952.

[28] BERTORELLE F, RUSSIER-ANTOINE I, CALIN N, *et al*. $Au_{10}(SG)_{10}$: a chiral gold catenane nanocluster with zero confined electrons. optical properties and first-principles theoretical analysis [J]. *J. Phys. Chem. Lett.*, 2017, 8(9): 1979-1985.

[29] DEÁK A, SZABÓ P T, BEDNAŘÍKOVÁV, *et al*. The first solid-state route to luminescent Au(I)-glutathionate and its pH-controlled transformation into ultrasmall oligomeric $Au_{10\text{-}12}(SG)_{10\text{-}12}$ nanoclusters for application in cancer radiotherapy [J]. *Front. Chem.*, 2023, 11: 1178225.

[30] COMBY-ZERBINO C, BERTORELLE F, CHIROT F, *et al*. Structural insights into glutathione-protected gold $Au_{10\text{-}12}(SG)_{10\text{-}12}$ nanoclusters revealed by ion mobility mass spectrometry [J]. *Eur. Phys. J.* D, 2018, 72(8): 144.

[31] MAITY S, BAIN D, PATRA A. Engineering atomically precise copper nanoclusters with aggregation induced emission [J]. *J. Phys. Chem.* C, 2019, 123(4): 2506-2515.

[32] GOSWAMI N, YAO Q F, LUO Z T, *et al*. Luminescent metal nanoclusters with aggregation-induced emission [J]. *J. Phys. Chem. Lett.*, 2016, 7(6): 962-975.

[33] WU Z N, YAO Q F, CHAI O J H, *et al*. Unraveling the impact of gold(I)-thiolate motifs on the aggregation-induced emission of gold nanoclusters [J]. *Angew. Chem. Int. Ed.*, 2020, 59(25): 9934-9939.

[34] DENG H H, HUANG K Y, XIU L, *et al*. Bis-schiff base linkage-triggered highly bright luminescence of gold nanoclusters in aqueous solution at the single-cluster level [J]. *Nat. Commun.*, 2022, 13(1): 3381

[35] ZEMAN C J, KIM S, ZHANG F, *et al*. Direct observation of the reduction of aryl halides by a photoexcited perylene diimide radical anion [J]. *J. Am. Chem. Soc.*, 2020, 142(5): 2204-2207.

[36] ZHOU M, JIN R X, SFEIR M Y, *et al*. Electron localization in rod-shaped triicosahedral gold nanocluster [J]. *Proc. Natl. Acad. Sci. USA*, 2017, 114(24): E4697-E4705.

汪琨钰(2000-),女,吉林长春人,硕士研究生,2021年于吉林大学获得学士学位,主要从事发光金属纳米团簇的研究。
E-mail: wky22@mails.jlu.edu.cn

张宇(1982-),男,吉林长春人,博士,教授,博士生导师,2010年于吉林大学获得博士学位,主要从事纳米光电材料与器件的研究。
E-mail: yuzhang@jlu.edu.cn

武振楠(1989-),男,安徽宿州人,博士,教授,博士生导师,2016年于吉林大学获得博士学位,主要从事金属纳米团簇发光材料与发光器件的研究。
E-mail: wuzn@jlu.edu.cn

白雪(1981-),女,吉林长春人,博士,教授,博士生导师,2008年于中国科学院长春光学精密机械与物理研究所获得博士学位,主要从事稀土纳米光电材料与器件的研究。
E-mail: baix@jlu.edu.cn